ISSN 0389-4010
UDC 519.27:
539.43:
620.168:

TECHNICAL REPORT OF NATIONAL AEROSPACE LABORATORY

TR-809T

Distributions of Fatigue Life and Fatigue Strength in Notched Specimens of a Carbon Eight-Harness-Satin Laminate

Toshiyuki SHIMOKAWA and Yasumasa HAMAGUCHI

May 1984

NATIONAL AEROSPACE LABORATORY

CHŌFU, TOKYO, JAPAN

Distributions of Fatigue Life and Fatigue Strength in Notched Specimens of a Carbon Eight-Harness-Satin Laminate*

by

Toshiyuki SHIMOKAWA** and Yasumasa HAMAGUCHI**

ABSTRACT

The objective of this research is to investigate the distribution properties of fatigue life and fatigue strength in sharply notched specimens of a carbon fabric laminate which was made of three layers of eight-harness-satin/epoxy prepreg sheets. Fatigue life distributions were obtained at six stress levels by carefully designed fatigue tests of four point plane bending under a constant temperature and humidity condition. Sample sizes were 30 for each of the three high stress levels and 12 for the three low stress levels. The amount of scatter and distributional form of fatigue life and fatigue strength are discussed from the test results. It is concluded that fatigue strength distributions are practically normal and their standard deviations are constant regardless of fatigue life.

概　要

本研究は炭素繊維８枚朱子織物／エポキシ樹脂３層積層材による鋭い切欠き試験片について疲労寿命と時間強度の分布特性を調べることを目的とする。温度と湿度を一定に保った実験室内において，実験の一様性に注意を払った４点平面曲げ疲労試験により，６応力レベルにおいて疲労寿命分布を導いた。使用した試験片の数は高応力側３レベルでそれぞれ30個，低応力側３レベルではそれぞれ12個である。得られた実験結果をもとに，疲労寿命と時間強度それぞれのばらつきの大きさと分布形状について検討する。この結果，実用的には時間強度の分布形は正規分布にあてはまり，標準偏差は疲労寿命によらないとみなせることを明らかにする。

INTRODUCTION

The application of advanced composites for aircraft structures is very actively being developed in the U.S.A., Europe, and Japan for the purposes of reducing structural weight, saving fuel, and improving payload and flight performance. Production parts made by advanced composites in civil aircraft are still limited to secondary structures. However, several prototypes of primary composite structures have been made and some of them are under flight testing.

These primary structures are of carbon/epoxy composites (CFRP). A lot of problems in using CFRP in production primary structure of civil aircraft have been left unsolved. CFRP's fatigue reliability is one of the most important problems, because composite structure is still difficult to be

* Received March 7, 1984

** Second Airframe Division

Presented at the Fourth International Conference on Composite Materials, ICCM-IV, held on Oct. 25-27, 1982, Tokyo, Japan.

produced so homogeneously as metallic structure. A few data with respect to the amount of scatter and distributional form of CFRP's fatigue life have been published [1-8]; however, total information available is quite insufficient. These data are of small sample size or limited to a narrow range of stress. The scatter of CFRP's fatigue life is generally much larger than that of aluminum alloy's fatigue life and its distributional form does not necessarily fit the log-normal or two-parameter Weibull distribution. In order to use CFRP in production primary structure of civil aircraft, much more information concerning fatigue life distribution should be accumulated.

In the present investigation sharply notched specimens of a carbon eight-harnes-satin/epoxy laminate, of which fatigue behavior is expected to be different from that of continuous fiber laminate specimens, were fatigue tested under plane bending. Their fatigue life distributions were obtained in a wide range of stress. This paper discusses five items: (1) fatigue damage accumulation and stiffness reduction, (2) fatigue life distributions, (3) the median S-N relation, (4) fatigue strength distributions and P-S-N curves, and (5) statistical comparison of fatigue life data obtained by five different panels cured separately. Some of these results are compared with those of 2024-T4 aluminum alloy [9], which is one of aircraft structural metals to be replaced by CFRP.

SPECIMEN AND METHOD OF TESTING

A carbon eight-harness-satin/epoxy laminate was made of three layers of Mitsubishi Rayon S 410 prepreg sheets with the lay-up sequence of (face/face/back) arranged in the same warp direction. Five laminate panels were manufactured at Mitsubishe Rayon, Ltd. on a hot press one by one under an identical cure cycle and trimmed to the size of 300 mm x 300 mm. Composite specifications and mechanical properties are listed in Table 1 and the cure cycle is in Table 2.

Figure 1 illustrates the specimen configuration. The theoretical stress concentration factors are approximately $K_b \doteqdot 3.8$ in plane-bending [10]

Table 1 Composite design specifications and mechanical properties.

Prepreg physical property[a]		Laminate[b] [3 plies in warp direc. (face/face/back)]			
Prepreg system	S 410 (8-harness-satin)	Property	Mean	c.v.[c]%	m[d]
		Thickness	1.14 mm	2.0	270
Ply thickness	0.40 mm	Tensile strength	612 MPa	2.1	5
Resin content	44±4 wt%	Tensile modulus	66 GPa	2.1	8
Mass/unit	720 g/m^2	Strain at failure	1.0 %	3.0	5
		Flexural modulus	77 GPa	1.9	7

[a]Catalogue data by Mitsubishi Rayon, Ltd.
[b]Produced by Mitsubishi Rayon, Ltd.
[c]Coefficient of variation.
[d]Sample size.

Table 2 Composite cure cycle.

Process	Pressure (kPa)	Temperature (°C)	Holding time (minute)
Cure	–	177	5
	686	177	120
Postcure	–	204	120

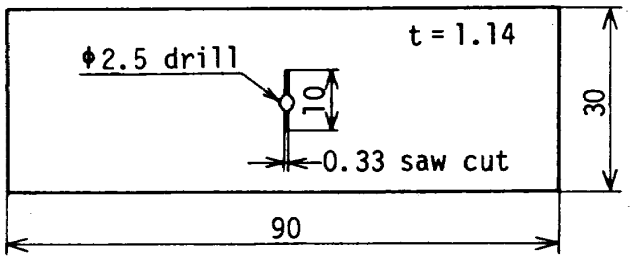

Fig. 1 Specimen configuration in millimeters.

and $K_t \fallingdotseq 8.7$ [11] in tension, which are calculated for a homogeneous isotropic elastic material with Poisson's ratio $\nu = 0.3$. The free test section is 30 mm long and its center is notched. Rectangular specimen blanks were machined by a diamond cutter, with warp direction longitudinal. The notch was first drilled 2.5 mm in diameter and cut with a fret saw machine having an electromagnetic exciter, with careful operation not to give any undesirable damage in the vicinity of the notch.

A conventional sub-resonant fatigue machine operating at a frequency of 30 Hz was employed. All fatigue tests with constant amplitude loading were performed by only one fatigue machine and one experimenter. Specimens were loaded in fully reversed plane bending by a four point bending fixture. This machine was driven by a synchronous motor and some overloads were originally observed during several seconds after the start of operation. In order to prevent these overloads, a flywheel of about 2.4 kg was attached directly to the motor and a brake was used during a few seconds after the machine was switched on. The overloads were completely removed by these devices. The electricity of constant frequency and voltage supplied from a special power equipment having a quartz oscillator was used for driving the synchronous motor.

The temperature and relative humidity in the laboratory were kept within the ranges of 22 to 24°C and 50 to 55%, respectively. Other experimental conditions were carefully controlled not to cause additional scatter in fatigue life distribution.

TEST RESULTS AND DISCUSSION

Stress Amplitude Representation

Nominal stress amplitude S represented by

$$S = 6M/bt^2, \quad (1)$$

for a homogeneous isotropic elastic material, is used in this paper. M is the bending moment loaded to the specimen, b the net specimen width, and t the specimen thickness. The thickness of each specimen was measured and the moment was adjusted so as to give the fixed nominal stress amplitude to the specimen.

Fatigue Damage Accumulation and Stiffness Reduction

Fatigue damage accumulation in a specimen observed by the eye is as follows. The debonding of a warp and a weft in the surface fabric occurred at the notch tip at first. This debonding stopped at the crossover section of both tows, where a warp passed under a weft. The debonding of this type propagated gradually warp by warp in the weft direction, and macroscopically, the damaged area was formed as a delta from the notch tip with the top of the delta to the side of the specimen. This behavior was observed on both sides at the notch tips. This damage accumulation reduced the stiffness and increased the strain amplitude in the net section. When this strain reached the strain limit of the specimen, fibers fractured suddenly and the specimen fractured at the same time. In the tests the propagation of delamination could not be confirmed and the gradual propagation of fiber fractures was not found. Fatigue failure based on the amplitude of the reciprocating platen of the fatigue machine reaching its limit due to the stiffness reduction of the specimen was not observed either. This kind of fatigue failure frequently occurred in a continuous fiber laminate [7]. Therefore, fatigue life is defined by specimen fracture in this paper.

Let the stiffness of a rectangular specimen without a notch for plane bending, namely, flexural rigidity, be EI. Figure 2 illustrates the

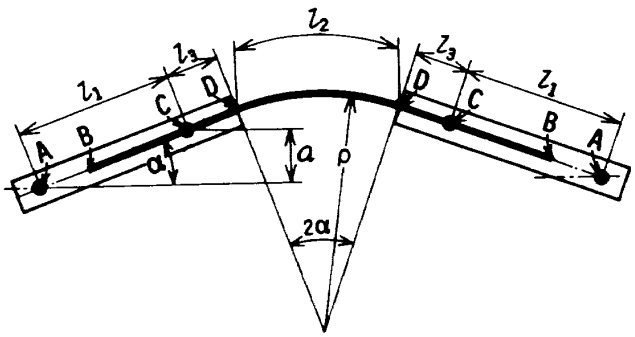

Fig. 2 Geometrical relation between the amplitude of the receprocating platen, a, and the radius of curvature of the deflected rectangular smooth specimen, ρ.

geometrical relation between the amplitude of the reciprocating platen of the fatigue machine, a, and the radius of curvature of the deflected specimen, ρ. In Figure 2, ℓ_2 is the test section of the specimen, the part BD of the specimen is clamped to the jig, and A is a fixed pivot point. The vibration of the reciprocating platen is loaded to the specimen at the pivot point C. As a uniform bending moment M is given to ℓ_2,

$$M/EI = 2\sin^{-1}(a/\ell_1)/\ell_2, \tag{2}$$

where ℓ_1 is AC, the residual stiffness ratio $EI/(EI)_o$ can be represented as

$$EI(EI)_o = \sin^{-1}(a_0/\ell_1)/\sin^{-1}(a/\ell_1) \doteqdot a_0/a. \tag{3}$$

Sub-zero means "at the start of testing". From the values of ℓ_1, a_0, and a given and obtained in this study, the right side of Equation (3) approximates the central function of Equation (3), the strict solution, in one percent error in the range of a_0/a larger than 0.6. The residual stiffness ratio of the approximate solution is used as the measure of the fatigue damage accumulation in the notched specimen in this study.

Figure 3 illustrates the residual stiffness ratio $EI/(EI)_0$ versus the cycle ratio n/N obtained at six stress levels, where n is the number of stress cycles and N the number of cycles to failure. The stiffness of specimen decreases a few percent within 5% of the specimen life, followed by a slow, linear reduction by about 20% until approximately 90% of the specimen life, and then a quick reduction to fracture. The residual stiffness ratio of 70% is judged to be just before the specimen fracture. Figure 3 shows that the relationship between the residual stiffness ratio and the cycle ratio is independent of stress level. This property is favorable in using a specific stiffness reduction ratio as a design criterion.

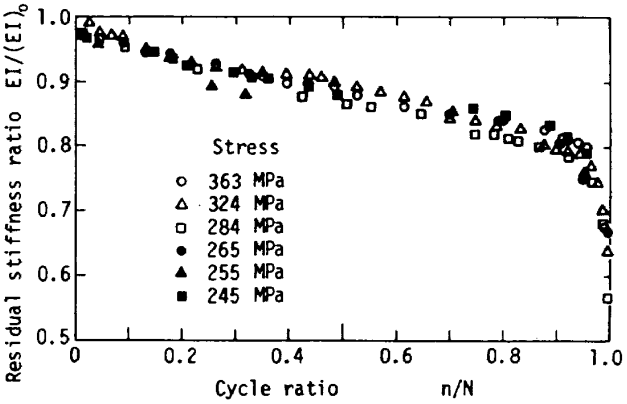

Fig. 3 Stiffness reduction versus cycle ratio.

Fatigue Life Distributions

Fatigue life tests were conducted at six stress levels. Sample sizes denoted by m are 30 for the three high stress levels, i.e., S=363(37.0), 324(33.0), and 284(29.0) MPa(kgf/mm^2), and 12 for the three low stress levels, i.e., S=265(27.0), 255(26.0), and 245(25.0) MPa(kgf/mm^2). At each stress level nearly equal number of specimens were randomly selected from each of the five laminate panels, A, B, C, D, and E. The test results of fatigue life N are listed in Table 3 and presented in Figure 4 on log-normal and Weibull probability paper. The plotting positions in Figure 4 are the median ranks. It is necessary to use the same plotting positions in comparing the goodness-of-fit of the two distribution models. Table 4 lists the median fatigue life and the estimated parameters for the log-normal and two-parameter Weibull distributions. In the log-normal distribution the parameters were estimated by the moments method for complete samples and by a graphical technique, i.e., the median ranks and the least squares method, for an imcomplete sample. In the two-parameter Weibull distribution the latter graphical technique was used.

Table 3 Fatigue life data of notched 8HS-3-ply specimens.

No.	S 363 MPa	P	S 324 MPa	P	S 284 MPa	P	S 265 MPa	P	S 255 MPa	P
1	25,300	E	137,800	D	530,500	D	2,491,700	A	3,752,300	C
2	30,000	D	142,400	E	659,400	D	2,733,100	B	4,128,400	E
3	35,100	E	143,800	E	674,400	E	2,855,000	B	4,971,400	E
4	37,800	D	144,400	C	694,100	E	3,474,200	C	6,386,200	E
5	42,400	D	147,200	B	718,800	A	3,508,200	D	8,395,200	B
6	42,600	D	152,000	D	739,600	E	3,638,200	A	9,037,700	D
7	42,900	E	152,700	E	866,200	E	3,971,300	C	10,328,000	C
8	44,400	E	165,900	E	891,900	D	4,169,700	E	10,793,400	D
9	45,100	C	191,600	E	920,100	D	5,359,100	C	11,275,700	D
10	48,200	D	194,000	E	931,200	B	5,978,900	E	15,033,900	D
11	49,200	B	202,800	A	1,008,100	C	6,921,500	D	16,814,700	C
12	49,400	C	207,300	D	1,011,700	D	15,340,800	D	21,900,600	B
13	52,100	A	212,000	A	1,016,100	B				
14	56,100	C	217,400	A	1,031,600	D				
15	57,100	A	219,300	C	1,089,400	C				
16	59,600	E	225,800	D	1,106,900	C				
17	59,700	A	226,100	B	1,146,500	E				
18	62,700	A	228,900	A	1,176,100	E				
19	62,900	B	231,800	A	1,196,600	C				
20	63,700	C	244,100	C	1,201,400	E				
21	63,900	D	247,600	D	1,296,700	B				
22	66,100	B	251,500	C	1,385,000	A				
23	67,500	B	256,200	B	1,509,500	A				
24	67,900	A	275,800	D	1,525,700	B				
25	68,400	E	289,500	A	1,550,200	B				
26	72,800	C	316,600	C	1,596,700	C				
27	81,500	B	353,200	B	1,840,500	A				
28	85,700	C	440,600	C	2,002,200	C				
29	96,000	B	444,900	B	2,033,200	C				
30	116,400	B	526,000	B	2,096,500	B				

No.	S 245 MPa	P
1	3,410,000	A
2	5,561,700	E
3	6,426,200	A
4	13,573,600	B
5	13,576,600	D
6	15,646,900	C
7	17,386,300	B
8	17,438,400	C
9	18,584,500	D
10	*22,281,000	B
11	*22,519,500	E
12	*28,964,600	B

P=Panel, * No failure.

Table 4 Median fatigue life and estimated parameters.

Stress S (MPa)	Sample size m	Median life $\tilde{N}$	Log-normal		Weibull	
			Mean $\bar{x}$	Standard deviation σ_L	Shape parameter α	Scale parameter N_c
363	30	58 350	4.7438	0.1442	3.681	64 400
324	30	222 550	5.3516	0.1531	3.721	260 800
284	30	1 098 150	6.0455	0.1561	3.436	1 304 700
265	12	3 804 750	6.6405	0.2188	2.607	5 357 000
255	12	9 682 850	6.9512	0.2413	2.090	11 520 200
245	12(3)*	16 516 600	7.1755	0.3696	1.645	19 209 300

* Number of specimens which did not fail.

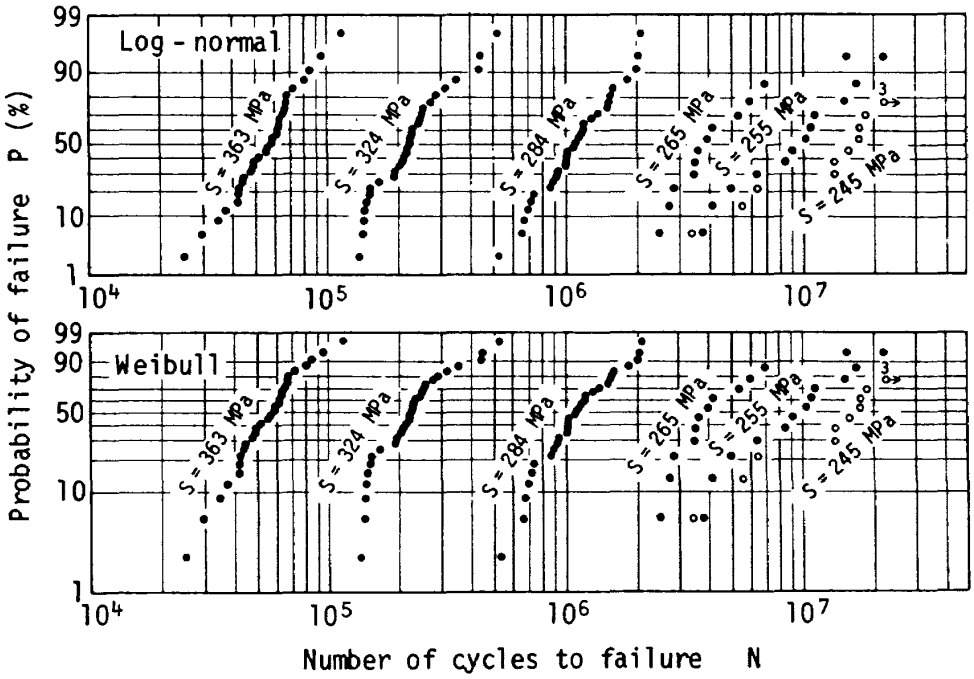

Fig. 4 Fatigue life distributions.

Distributional Form of Fatigue Life – The fatigue life distributions at the three high stress levels and S=255 MPa fit well with the log-normal distribution. The log-normal distribution is acceptable for the fatigue life distribution at S=265 MPa if the longest life is eliminated. Because of the three shortest lives, the fatigue life distribution at S=245 MPa fits better with the two-parameter Weibull distribution than the log-normal distribution. The Kolmogorov-Smirnov (K-S) and chi-square statistics for goodness-of-fit tests in Table 5 provide a comparison of relative goodness-of-fit of fatigue life data for the log-normal and two-parameter Weibull distributions. The K-S statistic verifies the tendency described above. The chi-square statistic for the data at the three higher stresses passes different judgments due to the number of cells, 5 or 6. This means that the sample size is not sufficient in these cases. Consequently, the log-normal distribution is generally better than the two-parameter Weibull distribution for the distribution model of fatigue life.

Table 5 Comparison of goodness-of-fit of fatigue life data for the log-normal and two-parameter Weibull distributions by the Kolmogorov-Smirnov and chi-square statistics.

Stress S (MPa)	Sample size m	Log-normal			Weibull		
		K-S	$\chi^2(5)^{a)}$	$\chi^2(6)^{a)}$	K-S	$\chi^2(5)^{a)}$	$\chi^2(6)^{a)}$
363	30	0.0967	3.67	2.40	0.1210	1.00	4.00
324	30	0.1216	4.00	6.40	0.1589	3.00	4.80
284	30	0.0800	4.00	0.80	0.1376	4.00	2.40
265	12	0.2039	–	–	0.2610	–	–
255	12	0.1218	–	–	0.1344	–	–
245	12(3)[b)]	0.2039	–	–	0.1815	–	–

a) Number of cells.

b) Number of specimens which did not fail.

Scatter of Fatigue Life – The amount of fatigue life scatter is measured by the standard deviation of log-life or the shape parameter of the two-parameter Weibull distribution, and their estimates, σ_L and α respectively, are listed in Table 4. The amount of fatigue life scatter is considered to be constant at the three high stress levels. The scatter at the three low stress levels is larger than that at the three high stress levels, and becomes larger as the stress level is lowered. The fatigue life scatter obtained in this paper is very small in comparison with that reported in Refs. [1-8].

Median S-N Curve

The median lives in Table 4 are plotted in Figure 5 on semi-logarithmic graph paper. The median S-N curve in Figure 5 is drawn by an eyeball fit.

The authors [9] have pointed out the empirical rule between the median S-N curve on semi-logarithmic graph paper and the distribution of fatigue life in an aluminum alloy as follows. The distributional form of fatigue life is closely related to the shape of the median S-N curve, namely, the distributional form of fatigue life is log-normal where the median S-N curve is practically linear, and its skew is pronounced where the slope of the median S-N curve changes rapidly. The amount of fatigue life scatter has a close relationship with the slope of the median S-N curve, i.e., the amount of fatigue life scatter is constant while the slope of the median S-N curve is equal, and becomes larger as the slope is gentler. The results at the three high stress levels and S=255 MPa fit well with this empirical rule. The agreement of the results at the other two low stress levels with this empirical rule is unclear. This may come from the small sample size. However, the empirical rule is effective in the sense that the amount of fatigue life scatter is larger than that at the three high stress levels due to the gentler slope of the median S-N curve.

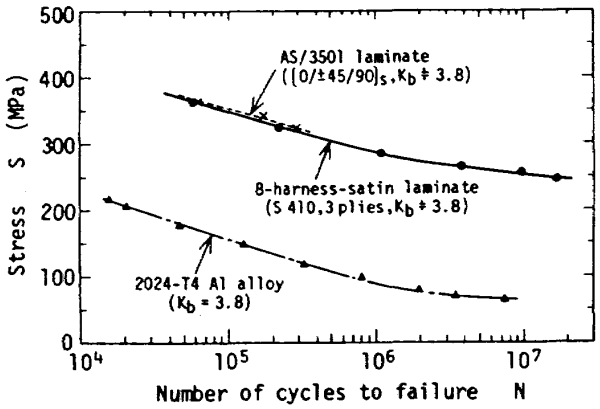

Fig. 5 Comparison of median S-N curves.

Figure 5 compares this median S-N curve with those of continuous carbon fiber composite specimens (AS/3501, 8-ply $[0/\pm45/90]_s$, $K_b \fallingdotseq 3.8$) [7] and aluminum alloy specimens (2024-T4, $K_b \fallingdotseq 3.8$) [9]. The difference in the median fatigue strength between the two composites is small and negligible. The median fatigue strength of the eight-harness-satin laminate is about 2.3 times at $N=10^5$, 3.2 times at $N=10^6$, and 4.0 times at $N=10^7$ as high as that of 2024-T4.

An analytical expression of the median S-N relation is necessary to discuss P-S-N curves in the next section. Figure 5 suggests that two straight lines in the high and low stresses can approximate well the median S-N data. The equations of the two straight lines are provided in Table 6.

Fatigue Strength Distributions and P-S-N Curves

The scatter of fatigue life in CFRP is very large, but that of fatigue strength is not so large in general. This means that in designing a CFRP

Table 6 Equation of the median S-N relation approximated by two straight lines on semi-logarithmic graph paper.

Stress range (MPa)	Life range (cycle)	Equation
380~280	3×10^4~1.2×10^6	S= –61.55 logN+655.0
280~240	1.2×10^6~ 2×10^7	S= –30.76 logN+468.1

structure for fatigue or planning its certification test fatigue strength can be more easily used than fatigue life. Therefore, fatigue strength distributions are derived from the fatigue life data, and P-S-N curves are determined.

As described before, at the three high stress levels the distributional form of fatigue life fit well with the log-normal distribution and the standard deviation of log-life is considered to be constant. Moreover, the median S-N relation in this stress range can be represented by a straight line on semi-logarithmic graph paper. It is clear from the P-S-N relation in this case that the distributional form of fatigue strength is normal and the standard deviation of fatigue strength σ_s is constant irrespective of fatigue life. The value of σ_s can be calculated from the slope of the median S-N curve h and the standard deviation of log-life σ_L as

$$\sigma_s = h\sigma_L, \qquad (4)$$

where h is taken to be absolute value. The standard deviation of log-life σ_L, which is considered to be constant regardless of stress level, is given in terms of the pooled variance of the measurements as

$$\sigma_L = \sqrt{\Sigma(m_i-1)\sigma_{Li}^2/\Sigma(m_i-1)}. \qquad (5)$$

σ_L is calculated to be 0.151 by using m_i and σ_{Li} values in Table 4. As h=61.55 from Table 6, Equation (4) provides σ_s=9.31 MPa.

Since at the three low stress levels the sample size is only 12 and the amount of fatigue life scatter is large, the fatigue life distributions obtained are not so simple as those at the three high stress levels. Consequently, instead of transforming the P-S-N relation, which are derived from fatigue life distributions, to fatigue strength distributions, the mean and standard deviation of fatigue strength are estimated by the Probit method [12]. This method involves the assumption that the fatigue strength distribution is normal. However, this assumption may have its validity as the extrapolation of the normal distribution of fatigue strength in the short life region corresponding to the three high stress levels. The mean and standard deviation are

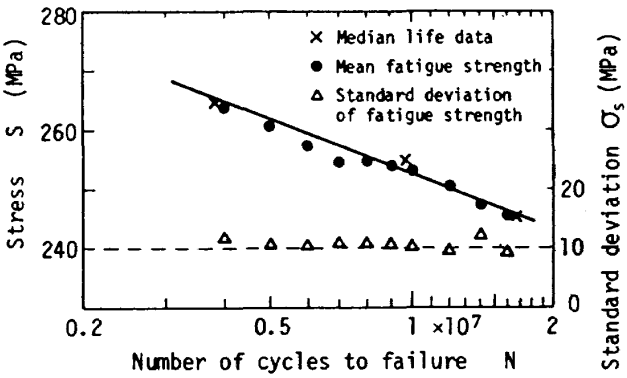

Fig. 6 Mean and standard deviation of fatigue strength estimated by the Probit method.

estimated by using the fatigue life data at the three low stress levels and plotted in Figure 6. Figure 6 also illustrates the median fatigue life data in Table 4 and the median S-N line drawn by the equation provided in Table 6. Figure 6 indicates that the means of fatigue strength agree well with the median S-N line, and the standard deviation of fatigue strength is about 10 MPa regardless of fatigue life.

As described above, the standard deviation of fatigue strength is about 9.3 MPa in the short life region and about 10 MPa in the long life region; therefore, 10 MPa is acceptable for the whole life region. The properties that the distribution of fatigue strength is practically normal and its standard deviation is constant regardless of fatigue life are similar to those of 2024-T4 aluminum alloy and desirable for engineering use. The standard deviation of 10 MPa is about 3 times that of 2024-T4 aluminum alloy. The coefficient of variation of fatigue strength of this fabric laminate is equal to or less than that of 2024-T4 for fatigue life larger than 10^6, because the median fatigue strength of this fabric laminate is more than 3 times that of 2024-T4 for this life region. The results described above and the comparison of the median S-N curves in the preceeding section prove this fabric laminate to be excellent as a substitute material for 2024-T4 aluminum alloy.

The P-S-N curves can be easily derived from the median S-N equation provided in Table 6 and the distribution model of fatigue strength, which

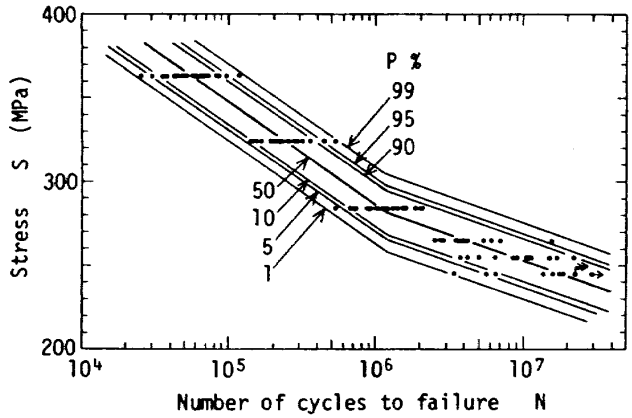

Fig. 7 P-S-N curves and fatigue life data.

is normal and has the standard deviation σ_s of 10 MPa regardless of fatigue life. Let the median S-N equation be S=f(N). Then the P-S-N relation corresponding to the probability of failure P is represented as

$$S_P = f(N) + u_P\sigma_s, \qquad (6)$$

Where u_p is the standard normal variable corresponding to P. Figure 7 illustrates the P-S-N curves derived and the fatigue life data. These P-S-N curves express the fatigue life data well and are considered to be sufficient for practical use.

Statistical Comparison of Fatigue Life Data Obtained by Five Different Laminate Panels

Five laminate panels used in the present investigation were produced one by one under the identical cure cycle. However, it is generally recognized that the qualities of CFRP have not been so homogeneously controlled as those of metals. Therefore, the fatigue life data obtained from the five different panels are statistically tested at 5% significance level to know whether there is any significant difference between the five panels. The fatigue life data used in the following discussion are those at the three high stress levels, because the sample size at these stress levels is fairly large and 4 to 7 specimens are selected from every panel for a series of fatigue tests at one stress level.

The log-life data obtained from the five panels, A, B, C, D, and E, are compared. The homogeneity of the five variances of log-life is tested by Bartlett's χ^2 test, the results of which are listed in Table 7. This homogeneity is accepted at the two stress levels except for that at S=324 MPa, which is accepted at 2.5% significance level. Figure 8 presents the mean S-N relations of the five panels, where the means are calculated on the basis of log-life. Analysis-of-variance for single factor experiment given in Table 8 shows that there is the significant difference between the fatigue life data obtained from the five different panels at each of the three stress levels.

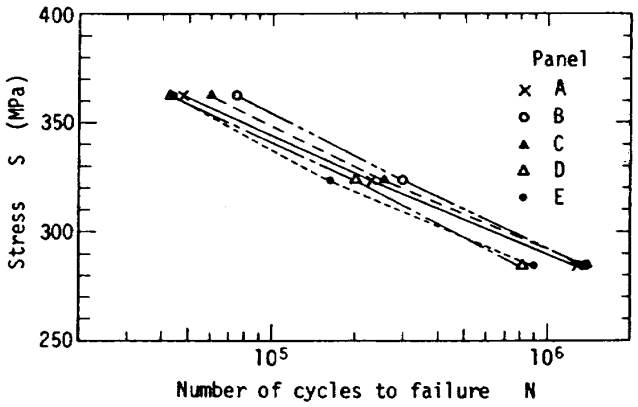

Fig. 8 Mean S-N relations of five different panels on log-life basis.

Table 7 Bartlett's χ^2 test for the homogeneity of log-life variances obtained from five different panels.

Stress S (MPa)	Bartlett's statistic χ_o^2	Critical values
363	5.31	χ^2 (4; 0.05)=9.49
324	11.0	χ^2 (4. 0.025)=11.14
284	0.975	

Table 8 Analysis-of-variance table for single-factor experiment of log-life data.

Stress S (MPa)	Source of variation SV	Sum of squares SS	Degrees of freedom DF	Mean square MS	Mean-square ratio MSR
363	Panels	0.266	4	0.0666	4.93
	Residual	0.337	25	0.0135	
	Total	0.603	29		
324	Panels	0.235	4	0.0589	3.31
	Residual	0.444	25	0.0178	
	Total	0.680	29		
284	Panels	0.285	4	0.0712	4.22
	Residual	0.422	25	0.0169	
	Total	0.707	29		

Minimum MSR required for factors to be significant at 95% confidence, $F(4,25;0.05)=2.76$.

In order to give the same nominal stress amplitude to every specimen in a series of tests at each stress level, the load was changed according to the specimen thickness. However, the difference in laminate thickness is considered to be a result of the difference in matrix volume. Hence, the measured data of laminate thickness in the five panels were compared. Though the thickness was measured at the net section and both sides of the notch, and the average value was used as the specimen thickness, the comparison was performed using every measured thickness. Bartlett's χ^2 test proved that the homogeneity of the five variances was accepted, but analysis-of-variance for single-factor experiment showed that there was the significant difference between the thickness of the five panels. Then, the correlation between specimen thickness and log-life was investigated with respect to each of the five panels and all of them. This correlation was rejected in every case at the three stress levels. Therefore, it is judged that there is no direct relationship between specimen thickness and log-life.

The results above and the fatigue damage accumulation behavior described before give an estimation that a significant difference in fatigue resistance by panels is produced from the difference in matrix conditions. It may be possible to improve the fatigue life scatter if the qualities of laminate panels are controlled more uniformly. Moreover, it should be emphasized that specimen allocation in fatigue tests is very important when two or more panels cured separately are used.

CONCLUSIONS

The distributions of fatigue life and fatigue strength in sharply notched specimens of a carbon eight-harness-satin laminate were investigated. The results obtained are as follows:

(1) According to visual observation on fatigue damage accumulation, the debonding of a warp and a weft in the surface fabric was pronounced, and the propagation of delamination was not confirmed. Fiber fractures were not found in the damage accumulation process and occurred at the final specimen fracture.

(2) The stiffness of a specimen decreased a few percent rapidly within 5% of the specimen life, and showed a slow, linear reduction by about 20% until approximately 90% of the specimen life, then quickly reduced to fracture. The relationship between the residual stiffness ratio and the cycle ratio was practically independent of stress level.

(3) The log-normal distribution was generally better than the two-parameter Weibull distribution for the distribution model of fatigue life.

(4) In the stress level range from S=284 to 363 MPa, the fatigue life scatter was invariant

and the standard deviation of log-life was roughly 0.15. The amount of fatigue life scatter obtained in the present paper was generally very small in comparison with the data of CFRP reported in Refs. [1-8].

(5) The empirical rule between fatigue life distributions and the median S-N curve on semi-logarithmic graph paper pointed out for an aluminum alloy fits the test results fairly well.

(6) Fatigue strength distributions in the short life region corresponding to the three high stress levels were of normal with the standard deviation of about 9.3 MPa and independent of fatigue life. In the long life region corresponding to the three low stress levels, the standard deviation of fatigue strength estimated by the Probit method was about 10 MPa regardless of fatigue life.

(7) The P-S-N curves were drawn using the fatigue strength distribution model, which was a normal distribution with the standard deviation 10 MPa regardless of fatigue life, and the median S-N relation approximated by two straight lines on semi-logarithmic graph paper. They fit the fatigue life data well and were considered to be sufficient for practical use.

(8) The median fatigue strength was 2 to 4 times that of 2024-T4 aluminum alloy for the life range from 10^5 to 10^7. The standard deviation of fatigue strength was about 3 times that of 2024-T4 aluminum alloy.

(9) Analysis-of-variance for single-factor experiment indicated that there was significant difference between the five panels cured separately for fatigue life. The difference in specimen thickness, however, did not have any significant effect on fatigue life.

ACKNOWLEDGMENTS

The authors wish to express their hearty thanks to Mitsubishi Rayon, Ltd. for providing the material used in this study and to Dr. Eiichi Nakai, Former Director of the Second Airframe Division, Mr. Toshiyasu Furuta, Head of the Composite Structure Section, at the National Aerospace Laboratory, and Dr. Sakae Tanaka, President of the University of Electro-Communications for their friendly advice and constructive criticisms.

REFERENCES

1. Halpin, J.C., "Structure-Property Relations and Reliability Concepts," *J. Composite Materials*, Vol. 6, 1972, pp. 208–231.
2. Nakayasu, H., Maekawa, Z., Fujii, T., and Mizukawa, K., "Statistical Study on the Properties of Fatigue and Static Strength of Uni-Directional CFRP Subjected to Tensile Load," *Proc. 19th Japan Cong. Mat. Res.*, 1976, pp. 195–200.
3. Ryder, J.T. and Walker, E.K., "Ascertainment of the Effect of Compressive Loading on the Fatigue Life Time of Graphite/Epoxy Laminates for Structural Application," AFML-TR-76-241, WPAFB, 1976.
4. Yang, J.N. and Jones, D.L., "Statistical Fatigue of Graphite/Epoxy Angle-Ply Laminates in Shear," *J. Composite Materials*, Vol. 12, 1978, pp. 371–389.
5. Phillips, L.N. and Sturgeon, J.B., "Some Initial Fatigue Tests on All-Carbon Fabric Laminates," *Int. J. Fatigue*, Vol. 1, No. 2, 1978, pp. 66–68.
6. Yang, J.N., Miller, R.K., and Sun, C.T., "Effect of High Load on Statistical Fatigue of Unnotched Graphite/Epoxy Laminates," *J. Composite Materials*, Vol. 14, 1980, pp. 82–94.
7. Shimokawa, T. and Hamaguchi, Y., "Fatigue Life Distributions of Notched Graphite/Epoxy Composite Specimens," *J. Soc. Mat. Sci., Japan*, Vol. 30, 1981, pp. 373–379.
8. Park, W.J. and Kim, P.Y., "Statistical Analysis of Composite Fatigue Life," *Progress in Science and Engineering of Composites, Proc. ICCM-IV*, 1982, pp. 709–716.
9. Shimokawa, T. and Hamaguchi, Y., "Relationship Between Fatigue Life Distributions and S-N Curve of Sharply Notched Specimens of 2024-T4 Aluminum Alloy," *Trans. Japan Soc. Aero. Space Sci.*, Vol. 21, No. 54, 1979, pp. 225–237.
10. Murakami, Y. and Araki, S., "Application of Body Force Method to the Analysis of

Transverse Bending of Arbitrarily Shaped Thin Finite Plate with an Elliptical Hole or Notch," *Transactions of the Japanese Society of Mechanical Engineers, Series A*, Vol. 45, No. 397, 1979, pp. 998–1006.

11. Isida, M., "On the Tension of a Strip with a Central Elliptic Hole (Part I)," *Transactions of the Japanese Society of Mechanical Engineers, Section 1*, Vol. 21, No. 107, 1955, pp. 507–513.
12. Little, R.E., *Manual on Statistical Planning and Analysis*, ASTM STP 588, 1975, pp. 52–53.

TECHNICAL REPORT OF NATIONAL
AEROSPACE LABORATORY
TR-809T

航空宇宙技術研究所報告809T号(欧文)

昭和59年5月発行

発行所 航空宇宙技術研究所
東京都調布市深大寺町1880
電話武蔵野三鷹(0422)47-5911(大代表) 〒182
印刷所 株式会社 共進
東京都杉並区久我山5－6－17

Published by
NATIONAL AEROSPACE LABORATORY
1,880 Jindaiji, Chōfu, Tokyo
JAPAN

Printed in Japan